



PERGAMON

Chemical Engineering Science 56 (2001) 3491–3504

Chemical  
Engineering Science

www.elsevier.nl/locate/ces

# A fundamental model of platinum impregnation onto alumina

W. A. Spieker, J. R. Regalbuto \*

*Department of Chemical Engineering, University of Illinois at Chicago, (MC 110), 810 S. Clinton Street, Chicago, IL 60607-7000, USA*

Received 6 July 2000; received in revised form 28 January 2001; accepted 12 February 2001

## Abstract

Refined forms of the revised physical adsorption Model (RPA) proposed by Agashe and Regalbuto (J. Coll. Interf. Sci. 185 (1997) 174) and a proton transfer model by Park and Regalbuto (J. Coll. Interf. Sci. 175 (1995) 239) were employed to model five sets of data of platinum (from chloroplatinic acid, CPA) adsorption over alumina found in the literature. Through a detailed individual consideration of ionic strength, which is the main cause of adsorption retardation at pH extremes, the results were further improved such that adsorption could be predicted a priori to a very reasonable degree without adjustable parameters. A comprehensive simulation of uptake as a function of initial platinum concentration, initial solution pH and the surface loading (amount of oxide surface per solution volume) shows that the model reflects all important features of adsorption typically seen in experimental studies and illustrates how it can be used to optimize the design of a catalyst impregnation. Over a range of low–moderate surface loadings corresponding to wet impregnation of relatively small amounts of oxide in excess solution, the diprotic chloroplatinic acid itself creates favorable electrostatic conditions and little or no pH adjustment is required to obtain full uptake of the available platinum from the solution (high “uptake efficiency”). At higher surface loadings corresponding to dry impregnation or pore volume filling that are more representative of industrial catalyst preparation recipes, however, the pH buffering effect of the oxide becomes so pronounced that additional acid is required to sufficiently charge the oxide surface and facilitate full platinum uptake. This offers a new interpretation of the often-cited necessity of excess hydrochloric acid in pellet impregnation at high surface loading, where a homogeneous metal distribution in the pellet is desired; the protons rather than the chloride ions may be the important factor. Furthermore, excessive amounts of platinum in solution (corresponding to an excess of a monolayer of Pt complexes at the surface) lead to self-inhibition based on high ionic strength in the solution and a dramatic drop in noble metal efficiency. © 2001 Elsevier Science Ltd. All rights reserved.

*Keywords:* Adsorption; Modeling; Simulation; Impregnation; Catalyst; Platinum

## 1. Introduction

The first step in the preparation of many heterogeneous catalysts is the process of impregnation, whereby metal complexes dissolved in aqueous solution are contacted with a porous oxide catalyst support such as alumina ( $\text{Al}_2\text{O}_3$ ) or silica ( $\text{SiO}_2$ ). During a contact time of typically an hour the noble metal adsorbs from an aqueous solution onto the high surface area support. The system can then be filtered, if excess solution has been employed, and the catalyst dried and further pretreated to transform the metal from its precursor state into its active form.

In such fashion catalysts are created in which the active phase is well dispersed as nanometer-scale, strongly anchored (hydrothermally stable) particles.

Historically, fundamental studies of catalyst preparation began with attempts to understand how to control the profile of metals placed into formed catalyst particles. Many earlier experimental studies (Maatman, 1959; Heise & Schwarz, 1987, 1990; Papageorgiou, Price, Gavriilidis, & Varma, 1996; Luengo, Sermon, & Sing, 1987) and theoretical models (Vincent & Merrill, 1974; Summers & Ausen, 1978; Heise & Schwarz, 1985, 1988; Lee & Aris, 1985; Ruckenstein & Karpe, 1989; Szeica, Castro, Dario, & Parera, 1986; Chu, Peterson, & Radke, 1989; Huang, Barrett, & Schwarz, 1986) attempted to describe this “adsorption–diffusion” process. In many of the latter, relatively simple adsorption mechanisms were

\* Corresponding author. Tel.: +1-312-996-0288; fax: +1-312-996-0808.

E-mail address: jrr@uic.edu (J. R. Regalbuto).

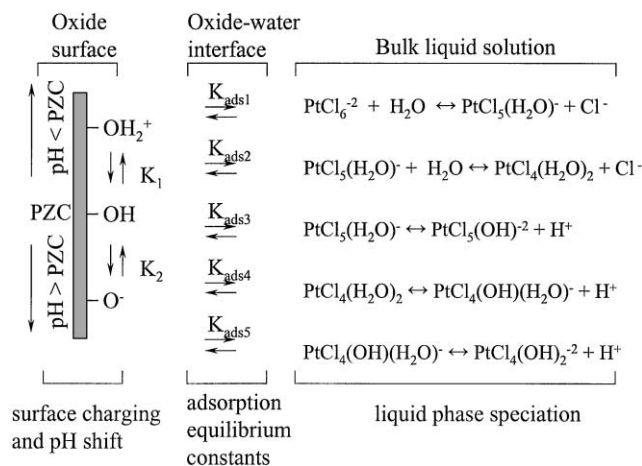


Fig. 1. Three regimes of a catalyst impregnation system.

invoked to keep the mathematics tractable. An exception was the paper of Ruckenstein and Karpe (1989), who invoked a more detailed accounting of solution nonideality and coulombic effects in his calculation of adsorption equilibrium constants. Over the last two decades, attempts to “transform the art of catalyst preparation into a science” have focussed more closely on the process of adsorption. Among the earlier works aimed at scientifically describing metal complex adsorption are the hallmark paper of Brunelle (1978), which qualitatively described the coulombic nature of noble metal complex adsorption onto common support oxides, the pioneering series of Heise & Schwarz (1985, 1986, 1987, 1988, 1990) on Ni/Al<sub>2</sub>O<sub>3</sub> and Pt/Al<sub>2</sub>O<sub>3</sub>, and the comprehensive, semiquantitative study of Pd/Al<sub>2</sub>O<sub>3</sub> by Contescu and Vass (1987).

To isolate adsorption from diffusion, well-stirred solutions containing metal precursors can be contacted with finely ground oxide support powders. Since typical values of electric double layer thickness are less than typical average pore radii, even for high surface area supports (Agashe & Regalbuto, 1997), a planar geometry can be assumed. A schematic of such an impregnation system is shown in Fig. 1. Three regimes have been delineated; the first describes the solution chemistry of the metal precursor in the bulk liquid. The formation of different species with potentially different charges must be modeled as a function of pH and other concentrations. The second regime describes the oxide surface and the charge that develops at its surface as a function of the solution pH. The oxide–water interface is the third regime. It is characterized through the adsorption equilibrium constants for each of the different metal species in solution. It is this regime, i.e. the nature of the adsorption step that distinguishes most of the adsorption models found in the literature.

There are three main variations of mechanisms which describe catalyst impregnation. These include a “coor-

dination chemistry” model, proposed for hydrotalcite-forming materials such as Ni–Al<sub>2</sub>O<sub>3</sub> (D’Espinoza de la Caillerie, Kermarec, & Clause, 1995), and echoed in several studies of Pt/Al<sub>2</sub>O<sub>3</sub> (Xidong, Yongnian, & Jiayu, 1988; Santacessaria, Carra, & Adami, 1977). According to this mechanism, adsorption of the hexachloroplatinate anion can only proceed subsequent to its complexation with dissolved aluminum. Secondly, there have appeared a number of quantitative “triple layer” models pertaining to catalyst impregnation (Mang, Breitscheidel, Polanek, & Knözinger, 1993; James & Healy 1972c) particularly those of Lycourghiotis’ group (Karakonstantis, Bourikas, & Lycourghiotis, 1996 and many earlier references). These parameter-laden models are based on presumed chemical interactions between the metal complexes and the oxide surface. Mechanisms of this sort (“triple layer”, “surface complexation”, “site binding”, etc.) can be referred to collectively as “chemical adsorption” mechanisms. The third variety of mechanism can be termed a “physical adsorption” mechanism, as it is based on purely physical (coulombic and solvation) and not chemical interactions. The physical adsorption model of James & Healy (1972a–c) was in fact one of the earliest quantitative adsorption models. Their original model contained an overestimation for the solvation energy, and compensated for this with an adjustable “chemical” energy term. That the magnitude of the adjustable term was so large may explain the eventual abandonment of this model (Brunelle, 1978) in favor of the phenomenologically more complex and more parameter-laden “chemical” models.

Motivated by such works as Brunelle’s, our work has centered on experimentally verifying a physical adsorption mechanism for noble metals to the exclusion of the coordinative and chemical models (Shah & Regalbuto, 1994; Santhanam, Conforti, Spieker, & Regalbuto, 1994; Regalbuto, Navada, Shadid, Bricker, & Chen, 1999), and revising the original model of James & Healy for the quantification of this mechanism (Agashe & Regalbuto, 1997). In an earlier paper we applied a preliminary version of the revised physical adsorption (RPA) model to all extent sets of data on CPA adsorption onto alumina (Regalbuto, Agashe, Navada, Bricker, & Chen, 1998), and obtained reasonable fits given that no parameters were adjusted in fitting the five sets of data. In the current work we more comprehensively apply a refined version of the parameter-free RPA model to all available sets of CPA/Al<sub>2</sub>O<sub>3</sub> adsorption data. The model validated in this way, we then present a number of generalized calculations that capture the main features of most alumina impregnations with CPA. We also demonstrate how these calculations might aid in the design of such impregnations. Specifically, the simulation results point to an alternative interpretation of the often-cited need for an acid such as HCl to achieve a homogeneous platinum distribution in catalyst pellets.

## 2. Theory

The three different regimes shown in Fig. 1 are described in the RPA model as follows.

### 2.1. Bulk liquid solution: CPA speciation in solution

Chloroplatinic acid undergoes a series of hydrolysis reactions after dissociation in aqueous solution (Gmelin & Meyer, 1939; Anderson, 1975; Davidson & Jameson, 1965; Cox & Peters, 1970; Sillen & Martell, 1971; Mang et al., 1993). The most comprehensive set of equilibrium constants for the hydrolysis is given by Anderson (1975) and Sillen and Martell (1971) and is that depicted in Fig. 1. Their model allows for the exchange of two of the six chloride ligands in the fully dissociated complex for either water or hydroxyls resulting in the formation of predominantly doubly valent species. Other speciation mechanisms have been suggested, and in fact we are currently utilizing EXAFS to study the speciation of CPA solutions (Spieker, Regalbuto, Kropf, & Miller, in preparation). For the present paper we have assumed for all simulations that the adsorbing species is doubly valent, which concurs with our experimental experience to date (Regalbuto et al., 1999). We also assume that two chloride ions are released into the solution per Pt complex, which is the simplest way to represent our preliminary EXAFS data. The coordination chemistry of Pt has a significant effect on the ionic strength, as will be explained below.

### 2.2. The oxide surface: charging and pH shift

The surface charging of an oxide is described through proton transfer reactions at the amphoteric hydroxyl groups. In aqueous solution, these become protonated or deprotonated as a function of the pH, rendering the oxide surface positively charged at low pH and negatively charged at high pH.



The surface ionization reactions are described by the constants  $K_1$  and  $K_2$ . Along with the hydroxyl group density  $N_s$  [OH groups/area] and the dielectric constant  $\epsilon$  these parameters fully characterize the charging properties of a particular oxide. Park and Regalbuto (1995) have shown in detail how the Gouy–Chapman model of the electric double layer (Healy & White 1978; Healy, Yates, White, & Chan, 1977) combined with a proton balance on the liquid phase can be used to quantitatively predict dramatic shifts in pH caused when oxides are added to solutions. Typically, the charging properties of an oxide are reported in terms of the PZC ( $=1/2(\text{p}K_1 + \text{p}K_2)$ ) and the difference between the logarithms of the ionization con-

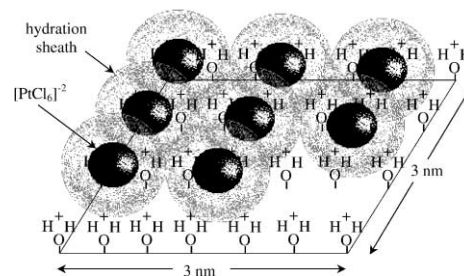


Fig. 2. Depiction of a closed packed layer of Pt complexes, retaining one hydration sheath, adsorbing over an oxide surface with about  $5 \text{ OH/nm}^2$ .

stants  $\Delta\text{p}K$  ( $=\text{p}K_2 - \text{p}K_1$ ). Both these parameters can be measured independently (James & Parks, 1982; Noh & Schwarz, 1990; Park & Regalbuto, 1995) and typical values for common metal oxides are cited in those papers.

### 2.3. The oxide–water interface: adsorption equilibrium constants

The RPA model employs a Langmuir adsorption isotherm for the metal ion adsorption density  $\Gamma$  [ $\text{mol/m}^2$ ] with the maximum density  $\Gamma_m$  determined to be a steric close-packed layer of adsorbates retaining one (for CPA) or two (for TAPC) hydration sheaths (Santhanam et al., 1994):

$$\Gamma = \Gamma_m \frac{KC}{1 + KC} \quad K = \exp\left(\frac{-\Delta G_{\text{ads}}}{RT}\right),$$

A depiction of the closed-packed metal complexes, adsorbed over a surface populated by about  $5 \text{ OH/nm}^2$ , is shown in Fig. 2. The hydrated complexes of  $[\text{PtCl}_6]^{2-}$  adsorb at a density of about  $1 \text{ complex/nm}^2$ .

The adsorption equilibrium constant  $K$  is then calculated a priori from a Gibbs free energy of adsorption  $\Delta G_{\text{ads}}$ , comprised solely of an attractive coulombic term  $\Delta G_{\text{coul}}$ . In James and Healy's (1972a–c) original model a so-called "chemical" energy term was added to coulombic and solvation terms as an adjustable parameter. Through the employment of a non-Nernstian description of the charge-potential relationship in the electric double layer adjacent to the oxide surface (Healy et al., 1977; Healy & White, 1978) and the solvation energy term by Levine (Wiese, James, & Healy, 1971), Agashe was able to significantly reduce the magnitude of the adjustable "chemical" energy term (in some cases to zero, Agashe & Regalbuto, 1997). In our latest, simplified version of the RPA model, we have found that the solvation term as well as the "chemical" term can be eliminated (Hao, Spieker, & Regalbuto, 2001). Thus for all simulations presented in this study, use of only the coulombic term for the free energy of adsorption renders a simplified model virtually free of adjustable parameters.

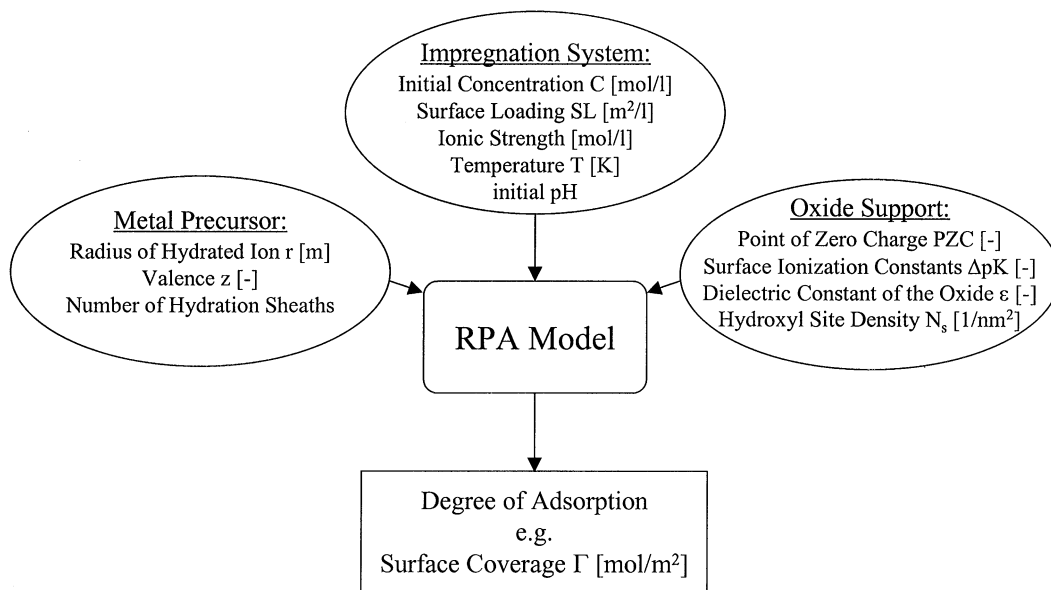


Fig. 3. “Black box” schematic of the combined RPA- and pH-Shift Model.

The following schematic (Fig. 3) summarizes the input required by the RPA algorithm. The calculations, which require the simultaneous solution of several equations and contain several levels of nested iterations, were done using the mathematics package Maple<sup>®</sup> V. For a full discussion of the model the reader is referred to the original publications of Agashe and Regalbuto (1997), Park and Regalbuto (1995), and especially Hao, Spieker, and Regalbuto (2001).

### 3. Results and discussion

#### 3.1. Essential features of the model

Fig. 4 illustrates how the surface charging, final pH, and Pt uptake vary, at constant metal concentration, as a function of solution pH over a  $\gamma$ -alumina surface under typical wet impregnation conditions. As the alumina is contacted with aqueous solutions, its surface hydroxyl groups become protonated at pH values less than its PZC, 8.5, and deprotonated at pH above 8.5, rendering the surface overall positively charged or negatively charged, respectively. As a consequence of this surface charge  $\sigma_0$ , an electric potential  $\psi$  builds up between the support surface and the adsorbing complex (Fig. 4a). The relationship between the charge and the potential is the focus of several electric layer theories (Yates, Levine, & Healy, 1974; Davis, James, & Leckie, 1978; James & Healy, 1972a–c); the RPA model utilizes the simple electric double layer (James & Healy, 1972a–c). The surface potential then serves as the driving force for the adsorption of ionic metal complexes that are present in the solution in a catalysis preparation system.

As shown in Fig. 4e, the proton transfer to the surface causes shifts in bulk liquid pH. Depending on the mass ratio of oxide to liquid, these shifts can be drastic and several pH units in magnitude (Mang et al., 1993; Regalbuto et al., 1998, 1999). The characteristic PZC of the oxide is manifested as the plateau of constant final pH in this figure. The width of the plateau indicating the PZC effectively depends on the surface loading ( $\text{m}^2/\text{l}$ ), which is the oxide mass loading ( $\text{g}/\text{l}$ ) multiplied by the surface area ( $\text{m}^2/\text{g}$ ). In so called dry impregnation with a very high oxide loading of for example  $150,000 \text{ m}^2/\text{l}$ , much larger pH shifts are observed than in wet impregnation where relatively small amounts of oxide (hundreds to thousands of  $\text{m}^2/\text{l}$ ) are contacted with the solution.

Adsorption of the anionic chloroplatinate complex ( $\text{PtCl}_6^{-2}$ , CPA) is predicted at pH values below the PZC, while adsorption of the cationic platinum tetraammine complex ( $(\text{NH}_3)_4\text{Pt}^{+2}$ , TAPC) occurs at pH values above the PZC (Fig. 4c). One of the main characteristics of this sort of plot is the adsorption maximum seen in either the chloride or amine complex. For either species, uptake increases as the pH moves away from the PZC of the support and the surface charge increases. In this simulation, the relative amounts of Pt and oxide surface were chosen such that monolayer adsorption of  $1.6 \mu\text{mol}/\text{m}^2$  for the chloride complex is almost attained. The doubly hydrated amine complex is larger and maximum monolayer adsorption corresponds to  $0.81 \mu\text{mol}/\text{m}^2$ . The larger size along with the relatively lower surface charge above the PZC (Fig. 4a) is the cause for the lower uptake of the amine complex (Fig. 4c). At either pH extreme, even while the alumina surface remains strongly charged one way or the other, Pt uptake falls precipitously. This

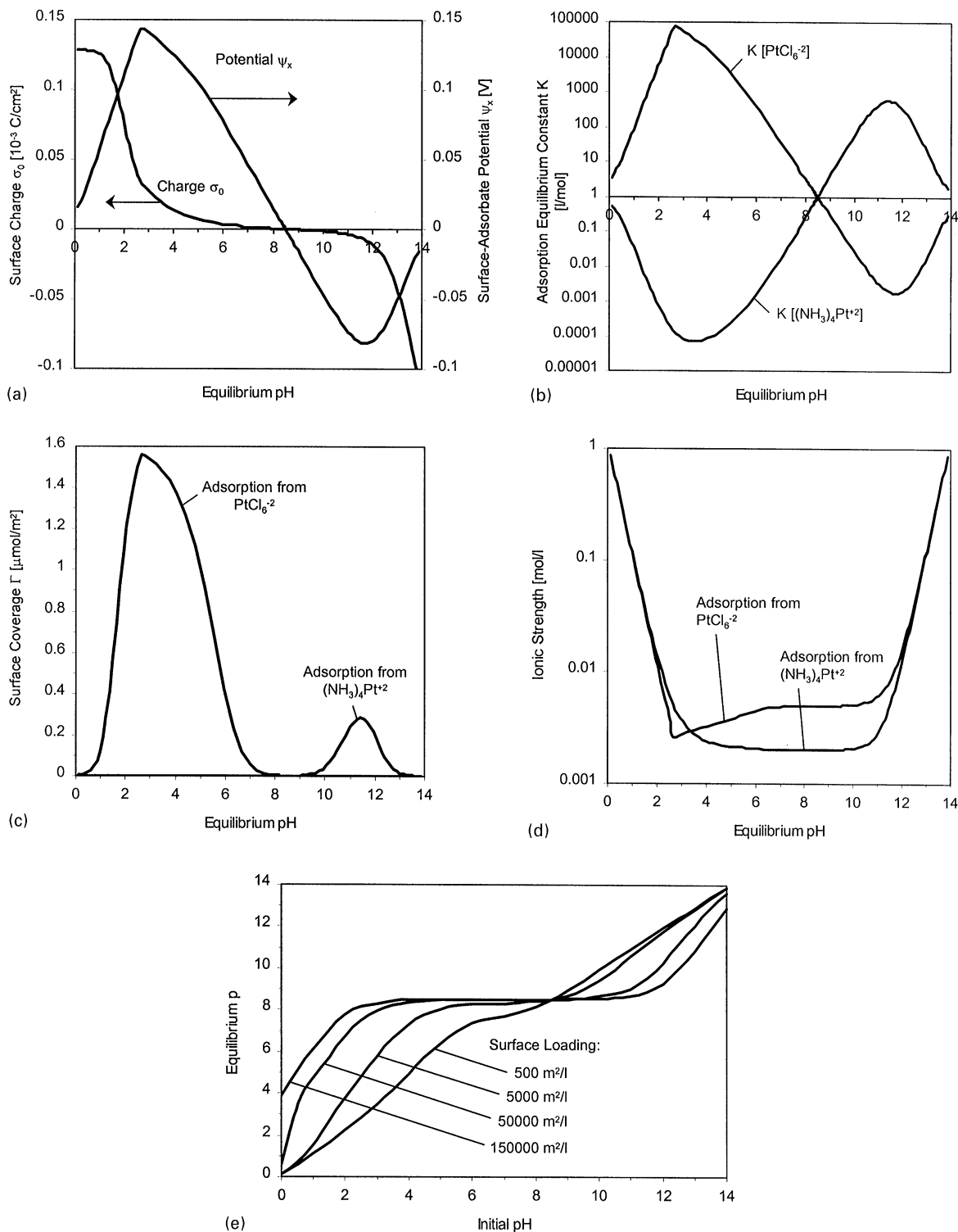


Fig. 4. Charging conditions, pH shift and adsorption in a platinum/alumina catalyst impregnation system.

phenomenon is based on the effect of high ionic strength (Fig. 4d), which causes the effective surface potential to diminish even in the presence of a strong surface charge (Fig. 4a). As a consequence, the RPA model predicts the adsorption constants (Fig. 4b) and thus the overall

uptake (Fig. 4c) to drop sharply, even in the absence of a “competitive” adsorbant like the often-cited Cl $^-$  (e.g. Mang et al., 1993; Smirnova, Belyi, Smolikov, & Dublyakin, 1990; Maatman, 1959). The surface is empty rather than filled with chloride ions.

While the pH itself presents the most important contribution to ionic strength, the significance of ionic strength warrants a more careful consideration of all factors contributing to it. The concentration of the platinum which remains in solution is another significant source. And at least three more effects can increase ionic strength to the extent that adsorption is significantly hindered. The first is the dissolution of the alumina support, which can become significant below a pH of about 3. For thermodynamic as well as kinetic reasons this effect is difficult to account for quantitatively. The solubility of different aluminas varies greatly with the phase and we found the dissolution process for  $\gamma$ -alumina usually not to be in equilibrium even after a period of 24 h (Regalbuto et al., 1999). Typical adsorption times in industrial catalyst preparation are much shorter (e.g. 1 h.) and the experimental data simulated in this study were taken after adsorption times between 1 and 6 h. For those cases where the aluminum concentration in the solution was measured and reported (Mang et al., 1993; Santacessaria et al., 1977), this effect can be accounted for.

The second source for increased ionic strength is the ligand exchange chemistry of the chloroplatinate species mentioned above. This process depends on the pH and likely also on the platinum concentration. In the absence of a comprehensive quantitative model of the CPA solution chemistry and in the light of varying experimental conditions in the simulated studies, the release of chloride ions into the solution through the ligand exchange process is in this paper assumed to be 2  $\text{Cl}^-$  per Pt complex.

The third effect on ionic strength stems from the counter ions from the adjustment of the initial pH, typically  $\text{Cl}^-$  or  $\text{Na}^+$  from hydrochloric acid or sodium hydroxide. The amount of acid or base needed to adjust the pH of a CPA solution can be significantly larger than expected due to the pH dependent ligand exchange process of the solution speciation, which partly “consumes” added protons or hydroxyl ions. This applies only to studies that investigate uptake as a function of initial solution pH like that of Mang et al. (1993). In order to simulate ionic strength in the system as realistically as possible, the simulation of the experimental data was conducted on an individual, point-by-point basis. For the general uptake surveys in the second part of the results, all of the above effects were accounted for except Al dissolution. It can be assumed that adsorption will be somewhat lower than predicted below pH 2 if highly soluble supports like  $\gamma$ -alumina are used at high oxide loading.

### 3.2. Modeling of experimental adsorption data

In this section we show the RPA model simulations of existing experimental data of platinum (CPA) adsorption over alumina supports. Five sets of quantitative data

were found in the literature with sufficient detail needed for the model. In four of the studies, adsorption isotherms were measured using varying Pt solution concentrations but leaving the pH unadjusted (Papageorgiou et al., 1996; Shyr & Ernst, 1980; Santacessaria et al., 1977; Jianguo, Jiayu, & Li, 1983). In the other (Mang et al., 1993) the solution pH was adjusted while the initial Pt concentration was left unchanged. (This is the manner in which we have conducted our own experiments (Regalbuto et al., 1998, 1999).) In the five data sets, different alumina phases in different physical shapes (powder, spheres or pellets) and with various surface areas were used. Table 1 in the appendix summarizes the important adsorption parameters of the studies. In all simulations a surface hydroxyl group density of 5 OH groups per  $\text{nm}^2$  and a  $\Delta\text{pK}$  value of 5, measured independently for alumina (Park & Regalbuto, 1995) was used. Unless the PZC was reported or could be inferred from reported pH-shift data (Mang et al., 1993), it was assumed to be 8.5 for all simulations. In all but one study (Mang et al., 1993) the final solution pH was not reported and the surface charging-proton balance portion of the RPA model was employed to estimate the final pH.

A complete and representative set of data of CPA adsorption as a function of pH is that of Mang et al. (1993). It features all the characteristics of the adsorption system as described above; pH shift with a plateau at the PZC (Fig. 5a) and adsorption of Pt anions below the PZC (Fig. 5b) with a maximum at pH 3. The ionic strength and the adsorption equilibrium constant (not shown) follow the trends displayed in Figs. 4b and d and explain the high ionic strength-induced retardation at lower pH. At the observed adsorption maximum the surface is only partially covered and the platinum is completely absorbed. Uptake of the entire amount of Pt initially in solution ( $0.005 \text{ mol/l}$ ) results at a surface loading of  $4540 \text{ m}^2/\text{l}$  in a surface coverage of  $(0.005 \text{ mol/l})/(4540 \text{ m}^2/\text{l}) = 1.1 \text{ } \mu\text{mol}/\text{m}^2$ , well below the steric maximum of  $1.6 \text{ } \mu\text{mol}/\text{m}^2$ .

A “chemical” adsorption theory was employed by Mang et al. (1993), and led them to conclusions very different from those of the RPA model. First, pH shifts were explained by the inclusion of adsorption reactions that involved exchange of surface hydroxyl groups. Second, the retardation at low pH was explained by competition from chloride ions. A careful experimental look at chloride uptake in the regime where Pt adsorption is inhibited indicated that no chloride is adsorbed (Regalbuto et al., 1999); these results are in agreement with the RPA mechanism, whereby the surface is not chloride-filled, but is simply empty.

The next several Figs. 6–9 refer to experiments wherein adsorption was measured as CPA concentration was increased, in the manner normally used to extract an adsorption constant from a Langmuir isotherm. The results are plotted in the originally reported format as

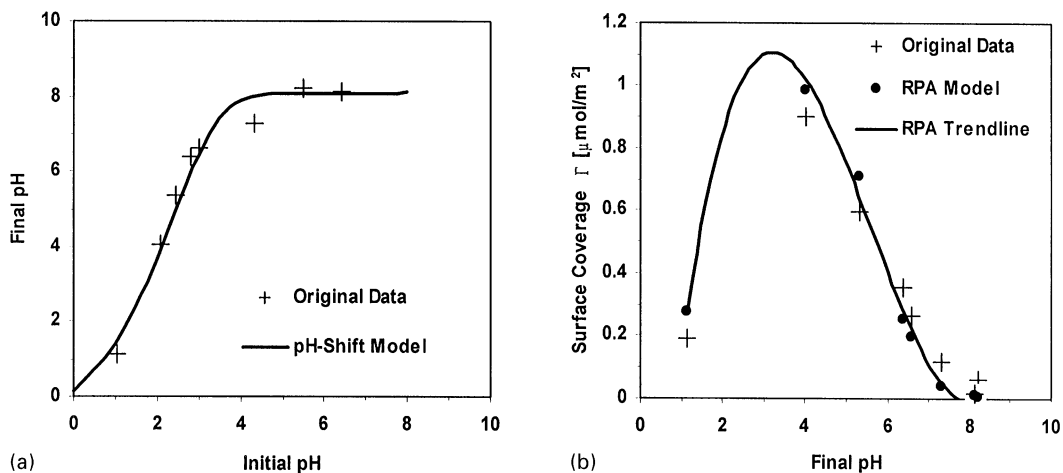


Fig. 5. Simulation of pH shift and platinum adsorption data of Mang et al. (1993), ( $SL = 4540 \text{ m}^2/\text{l}$ ,  $C_{\text{Pt,initial}} = 5 \text{ mmol}/\text{l}$ , contact time: 1 h).

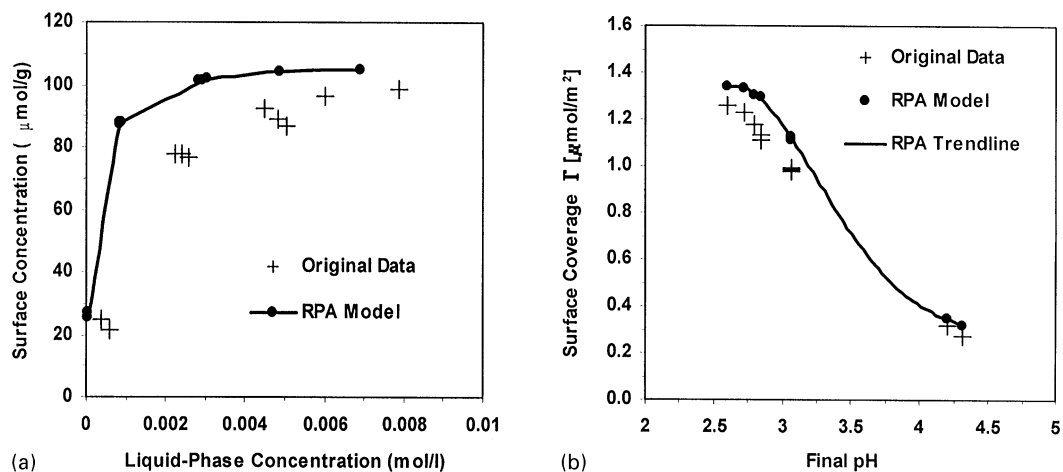


Fig. 6. Simulation of platinum adsorption data of Papageorgiou et al. (1996), ( $SL = 11\,760 \text{ m}^2/\text{l}$ ,  $C_{\text{Pt,initial}} = 0.4\text{--}7.9 \text{ mmol}/\text{l}$ , contact time: 1.5 h).

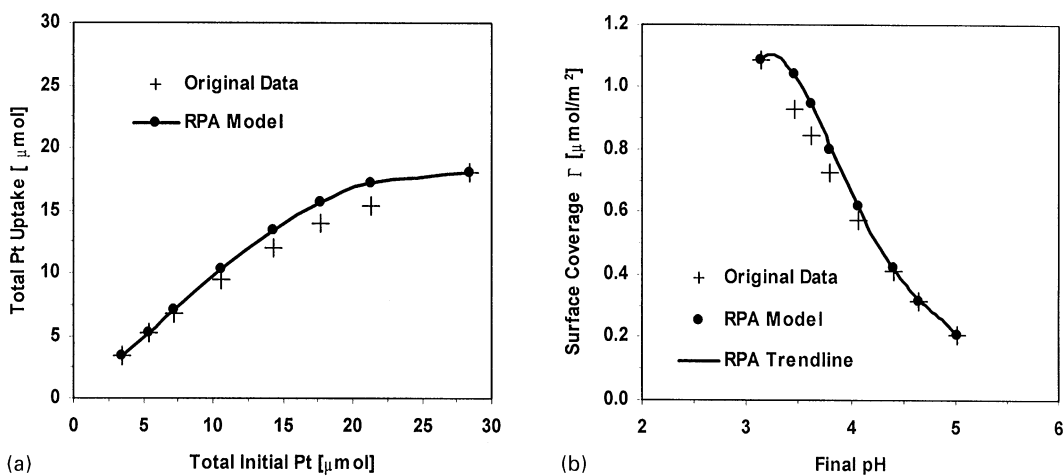


Fig. 7. Simulation of platinum adsorption data of Shyr and Ernst (1980), ( $SL = 33\,000 \text{ m}^2/\text{l}$ ,  $C_{\text{Pt,initial}} = 7\text{--}57 \text{ mmol}/\text{l}$ , contact time: 2 h).

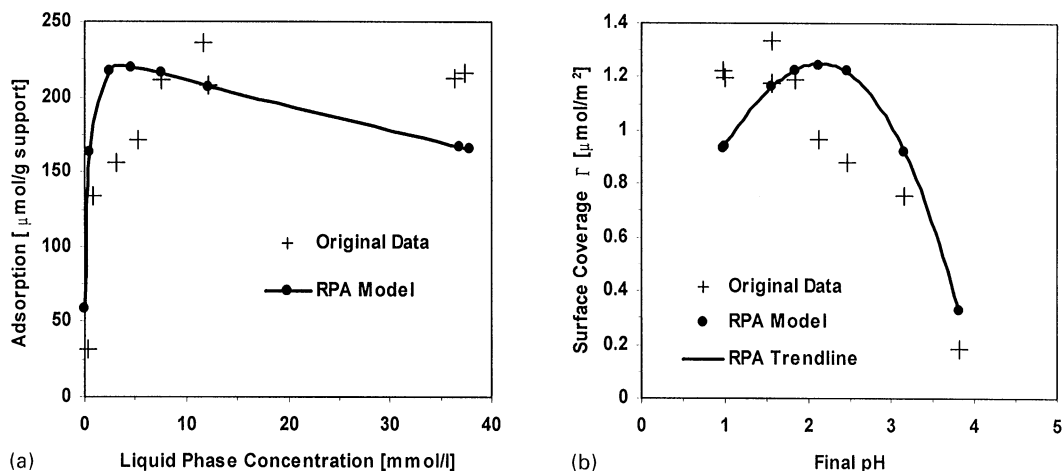


Fig. 8. Simulation of platinum adsorption data of Santacessaria et al. (1977), ( $SL = 2200 \text{ m}^2/\text{l}$ ,  $C_{\text{Pt,initial}} = 0.7\text{--}40 \text{ mmol/l}$ , contact time: 3–8 h).

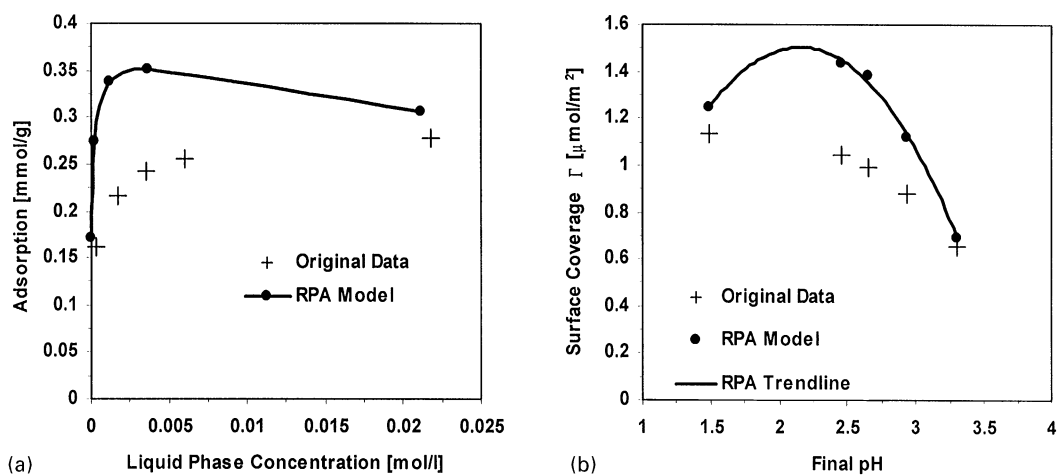


Fig. 9. Simulation of platinum adsorption data of Jianguo et al. (1983), ( $SL = 6125 \text{ m}^2/\text{l}$ ,  $C_{\text{Pt,initial}} = 4.3\text{--}29 \text{ mmol/l}$ , contact time: 6 h).

adsorption isotherms (Figs. 6a–9a) and also in terms of surface coverage versus final pH (Figs. 6b–9b).

In light of the RPA model results, the fitting of the adsorption isotherms in Figs. 6a–9a by a single equilibrium constant over the entire concentration range, as was done by Papageorgiou's group, is only a first approximation. The value they obtained from the data in Fig. 6a was 606 l/mol. For the 10 data points shown in Fig. 6b, the adsorption equilibrium constant as calculated with the RPA model varies from 9146 l/mol at the lowest concentration (lowest ionic strength) to 608 l/mol at the highest concentration. At first it may seem that the RPA model does not then utilize a Langmuir isotherm, since the equilibrium constants are a function of metal concentration and so indirectly a function of surface coverage. By including the Debye–Hückel effect in the adsorption equilibrium constants, we have chosen to follow the format of James & Healy. Alternatively, the adsorption-suppressing Debye–Hückel effect can be expressed as solution nonideality in

the form of activity coefficients as was done by Ruckenstein and Karpe (1989) and Heise and Schwarz (1985). Strictly speaking then the RPA model does employ a Langmuir isotherm, but also incorporates solution non-ideality.

It is interesting to note that the closest agreement with theory occurred for those studies, which employed the shorter contact time. Mang (Fig. 5) used 1 h, Papageorgiou (Fig. 6) used 1.5 h and Shyr (Fig. 7) used 2 h. Santacessaria (Fig. 8) used 3 to 8 h while Jianguo (Fig. 9) used 6 h. The longer contact times would have led to higher degrees of alumina dissolution, which in turn gives rise to higher ionic strength and thus retarded adsorption. Aluminum dissolution data was available only for Mang's and Santacessaria's study and the reason for the RPA simulation to fall below the experimental data at the extremely low pH values in Santacessaria's case is mainly due to assumed high ionic strength from Al dissolution. The sensitivity of Pt uptake ( $\Gamma$ ) to the

inclusion or omission of Al dissolution in the calculation of ionic strength was in general less than about 20%. Incidentally, evidence for Pt–Al bonds has not appeared in our preliminary EXAFS results (Spieker et al., in preparation), which suggests that the Pt–Al coordination complexes proposed by some (Xidong, Yongnian, & Ji-ayu, 1988; Santacessaria et al., 1977) at low pH are not present.

Another cause of the general trend of slight overestimation of adsorption by the RPA model can lie in the simplifying assumption of only doubly valent platinum species. Monovalent complexes, as they are predicted by some speciation models would experience weaker electrostatic attraction leading to an overall lower adsorption. Our current EXAFS studies on CPA coordination chemistry are aimed at providing the data for a comprehensive quantitative speciation model that should answer this question.

Besides the data sets shown above, we have in a previous work also simulated our own experimental data for many different phases of alumina ( $\gamma, \theta, \eta, \alpha$ ) and surface areas (28–220 m<sup>2</sup>/l) (Regalbuto et al., 1999). That adsorption was seen to be independent of aluminum dissolution ( $\alpha$  being sparingly soluble,  $\theta$  and  $\eta$  moderately so, and  $\gamma$  the most soluble), suggests that the coordination mechanism does not apply. The modeling results were sufficiently accurate that they are not reproduced here. Since all of these aluminas have similar PZCs, since Al dissolution is inconsequential to uptake, and since a common oxide loading of 500 m<sup>2</sup>/l was employed, all results fell roughly onto one curve and could be simulated with a single set of physical parameters.

In light of the widely varying parameters like surface area, surface loading and concentration range and the fact that the final pH and aluminum concentrations was not reported for many of these data sets, the RPA model using the same set of charging parameters simulates the experimental values reasonably well.

### 3.3. Comprehensive simulation and impregnation strategies for platinum adsorption over alumina

The following section shows a comprehensive simulation of platinum adsorption from CPA solution onto  $\gamma$ -alumina as a function of the solution pH and the initial platinum concentration. The calculations are performed at different surface loadings to illustrate a progression of conditions from wet to dry impregnation. Fig. 10, at 500 m<sup>2</sup>/l represents the situation of many of our benchtop adsorption experiments in which we add relatively little oxide to an excess of solution (say 0.125 g of a 200 m<sup>2</sup>/g alumina to 50 ml of solution). This is done in an attempt to minimize the pH shift of the solutions. A moderate surface loading, 5000 m<sup>2</sup>/l (Fig. 11) is representative of many adsorption studies performed in the literature, in-

cluding the data sets modeled in the previous section. Finally, 150,000 m<sup>2</sup>/l (Fig. 12) is representative of dry impregnation, or impregnation to incipient wetness, in which solution is added just to fill the pore volume of the solid support. This condition is perhaps closest to most industrial recipes.

Each calculation is presented as metal uptake or surface coverage  $\Gamma$  (in  $\mu\text{mol}/\text{m}^2$ ) versus initial concentration and equilibrium (final) pH (Figs. 10a–12a). The pH shifts are shown in Figs. 10b–12b, in which equilibrium pH is plotted as a function of initial pH and metal concentration, and in Figs. 10c–12c this effect is taken into account and metal uptake versus initial concentration and initial pH is plotted. The fraction of metal adsorbed, which might be considered the “uptake efficiency” is then plotted in Figs. 10d–12d. Given the high affinity of the Pt for the surface, utilization falls precipitously as soon as a liquid metal concentration roughly equivalent to a monolayer of metal is reached, for all surface loadings.

The dashed line on each surface represents the set of states produced by adding only CPA, which itself is a diprotic acid, in varying concentrations, to water. We refer to this as the loci of “intrinsic” states of the system. The higher pH section of the surface is brought about by addition of NaOH, while the lower pH surface is attained by addition of HCl to the various concentrations of CPA.

The features of the two dimensional results of Fig. 4 can be easily visualized in the three-dimensional surface of Figs. 10–12. In Fig. 10 since the surface loading is relatively low, the plots versus final and initial pH are only changed by a relatively small amount and the pH shifts are not too large. As explained earlier, uptake occurs at final pH values below the PZC of alumina (8.5) and falls off below a pH of about 2 due to ionic strength. Along a line of a constant pH favorable for strong adsorption, e.g. pH = 3, the surface completely absorbs all available platinum from a dilute solution and the coverage accordingly increases with increasing Pt concentration until a maximum of about 1.6  $\mu\text{mol}/\text{m}^2$  is reached. This corresponds to the aforementioned steric limit of a monolayer of close-packed hydrolyzed complexes on the surface. For a surface loading of 500 m<sup>2</sup>/l, this point is reached at an initial concentration of about 180 ppm Pt or 0.8 mmol/l ( $=500 \text{ m}^2/\text{l} \times 1.6 \mu\text{mol}/\text{m}^2$ ) and corresponds to about 4.5 wt% Pt on an alumina with a surface area of 150 m<sup>2</sup>/g. A further increase in platinum concentration beyond this value appears to be a waste of precious precursor metal, as the surface is not only “filled”, but the coverage falls again below the maximum due to the increase in ionic strength from the platinum itself. For this lowest loading, strong adsorption or high uptake efficiency (Fig. 10d) results from the CPA solutions themselves, without having to resort to any pH adjustment. In contrast, as we consider the highest surface loading (Fig. 12) we will see that the pH shift is so severe that

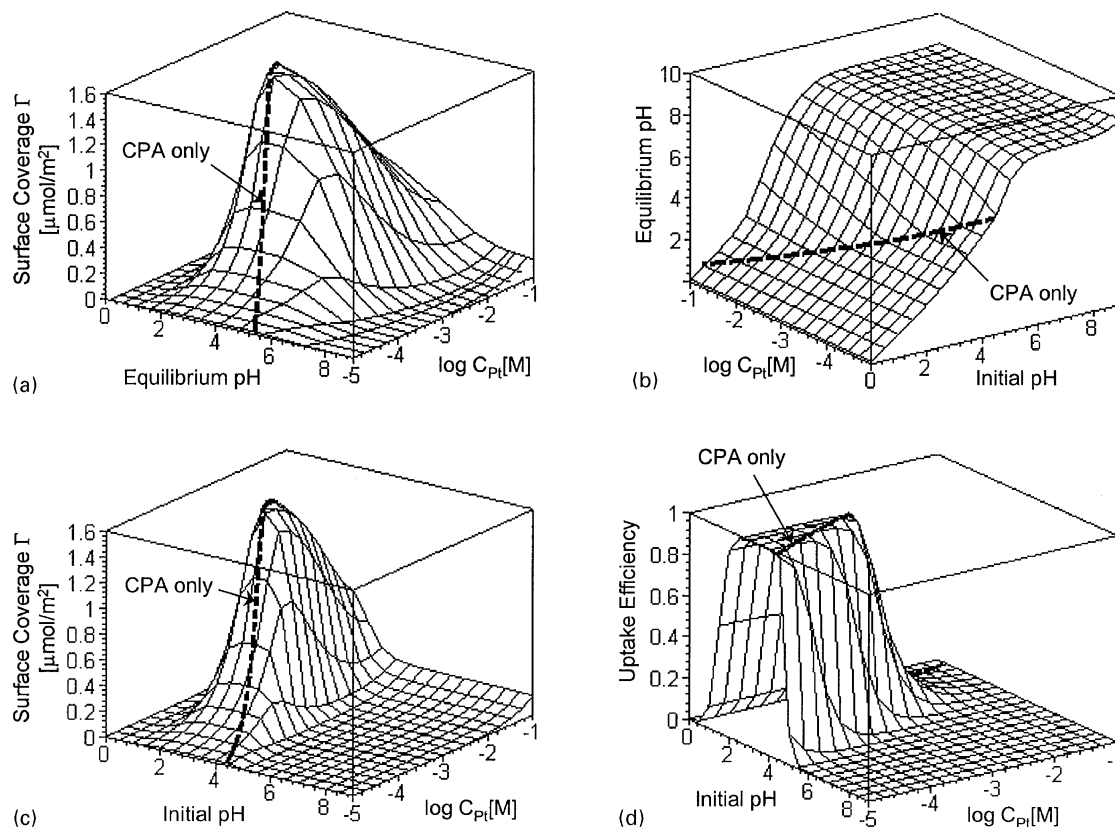


Fig. 10. Simulation of platinum adsorption and pH shift in a CPA/ $\gamma$ -alumina impregnation system at a surface loading of  $500 \text{ m}^2/\text{l}$ : (a) surface coverage vs. initial Pt concentration and equilibrium pH; (b) equilibrium pH vs. initial Pt concentration and initial pH; (c) surface coverage vs. initial Pt concentration and initial pH; (d) uptake efficiency vs. initial Pt concentration and initial pH.

acid must be added to sufficiently charge the surface at typically low metal loadings.

The moderate surface loading shown in Fig. 11 is typical of the literature studies we have simulated earlier. The five studies cited employed surface loadings ranging from 2210 to 33 000  $\text{m}^2/\text{l}$  (see Table 1). The two-dimensional curves seen in Figs. 5–9 can be traced (approximately, given the different surface loadings) onto Fig. 11. It is seen that the constant metal concentration—variable pH curve of Mang et al. (1993) that runs parallel to the pH axis is distinctly different from the other four studies, which follow the intrinsic state curve (labeled “CPA only”). Mang’s study exhibits the high ionic strength retardation effect, but never reaches monolayer loading as the metal concentration employed was too low. The study of Papageorgiou approaches the uptake maximum along the intrinsic pathway, but never reaches it, while the studies of Santacessaria, Shyr and Jianguo (the latter of which is indicated in the plot as it is representative of these three sets) extend beyond the uptake maximum and become “self-inhibited” by high ionic strength due to CPA itself. While with Mang and Papageorgiou, utilization of Pt at the respective observed uptake maximum is high (close to 100%), it is relatively low in the latter three studies (20, 24 and 37%, respectively).

The final set of computations represents a typical industrial surface loading, which is close to “incipient wetness”, or pore volume filling. Shifts in pH are quite pronounced (Fig. 12b) resulting in a great degree of widening of the plot of Fig. 12c into that of Fig. 12a. Very significantly, the locus of intrinsic states is far from optimal in terms of uptake efficiency (Fig. 12d). For example, if a metal loading of 0.1 wt% Pt is desired on a  $250 \text{ m}^2/\text{g}$  alumina catalyst, and impregnation is to occur to fill the pore volume of  $1 \text{ cm}^3/\text{g}$ , the final surface loading would be  $150,000 \text{ m}^2/\text{l}$ , at a Pt concentration of  $3.1 \text{ mmol/l}$ . An “x” in the four parts of Fig. 12 marks the conditions of this point. At this high surface loading, the number of hydroxyl groups on the alumina surface is large relative to the number of protons initially in solution. The surface consumes the majority of protons and remains relatively uncharged while driving up the pH. To get to the regime of strongest possible Pt-surface interaction, and presumably the highest final metal dispersion, acid must be added such that the new, optimal state, marked with a filled circle is obtained.

To achieve uniform metal profiles in industrial impregnations of formed catalysts, the need for an acid such as HCl is often cited (Maatman 1959; Mang et al., 1993; Smirnova et al., 1990). The common interpretation has

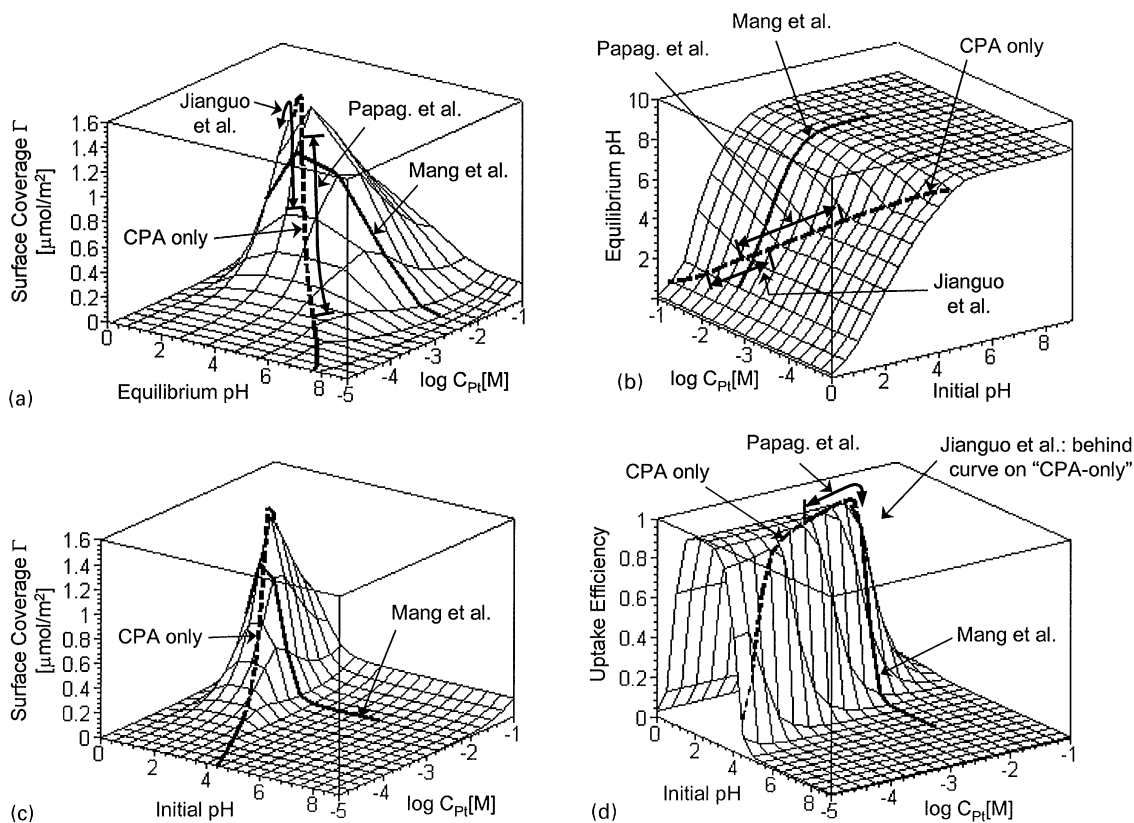


Fig. 11. Simulation of platinum adsorption and pH shift in a CPA/ $\gamma$ -alumina impregnation system at a surface loading of  $5000 \text{ m}^2/\text{l}$ : (a) surface coverage vs. initial Pt concentration and equilibrium pH; (b) equilibrium pH vs. initial Pt concentration and initial pH; (c) surface coverage vs. initial Pt concentration and initial pH; (d) uptake efficiency vs. initial Pt concentration and initial pH.

been that chloride or some other anion is needed to compete with the Pt complex for adsorption sites. In view of Fig. 12, the interpretation of the successful recipe is quite different. It is not the  $\text{Cl}^-$  from the HCl that is needed, but rather the protons, in order to charge the surface sufficiently for metal adsorption to occur. Without additional acid the interior of catalyst pellets will not become charged, and no adsorption will occur there. This new interpretation is supported by our previous experimental investigation, which revealed that  $\text{Cl}^-$  adsorption does not occur in the low pH regime of retarded Pt adsorption (Regalbuto et al., 1999). A more thorough study of formed catalysts is planned in the future.

The influence of the surface loading can be summarized by comparison of Figs. 10 and 12. Three major trends are observed as surface loading increases. First, the locus of the maximum coverage shifts toward higher initial Pt concentrations. This is logical since a higher absolute amount of surface in the system requires more platinum for the same surface coverage. Secondly, this locus shifts towards lower initial pH values. Figs. 10b and 12b illustrate that the pH buffering effect in the system increases with the surface loading. A larger pH shift during the impregnation requires the initial solution pH to be lowered even more in order to arrive at the same equilibrium

pH that is suitable for strong adsorption. Finally, the uptake efficiency of the CPA-only solutions starts to drop at lower Pt concentrations. This is also a consequence of the larger pH shifts; the acidity of the CPA solution itself is not sufficient to keep the solution pH in the range favorable for strong adsorption and the addition of acid becomes necessary at lower platinum concentrations.

#### 4. Conclusions

The RPA model can be used to describe the adsorption of platinum derived from CPA onto many types of alumina with different surface areas to a very reasonable degree without adjustable parameters. It was shown that the model accurately reflects all important features of adsorption as a function of the impregnation system parameters like initial platinum concentration, surface loading and pH. The good agreement between experimental and simulated data suggests that we have an understanding of the fundamental principles of platinum adsorption over alumina supports.

It was also demonstrated how the model can be used to optimize a catalyst impregnation with respect to either "noble metal efficiency" or maximum uptake. The results

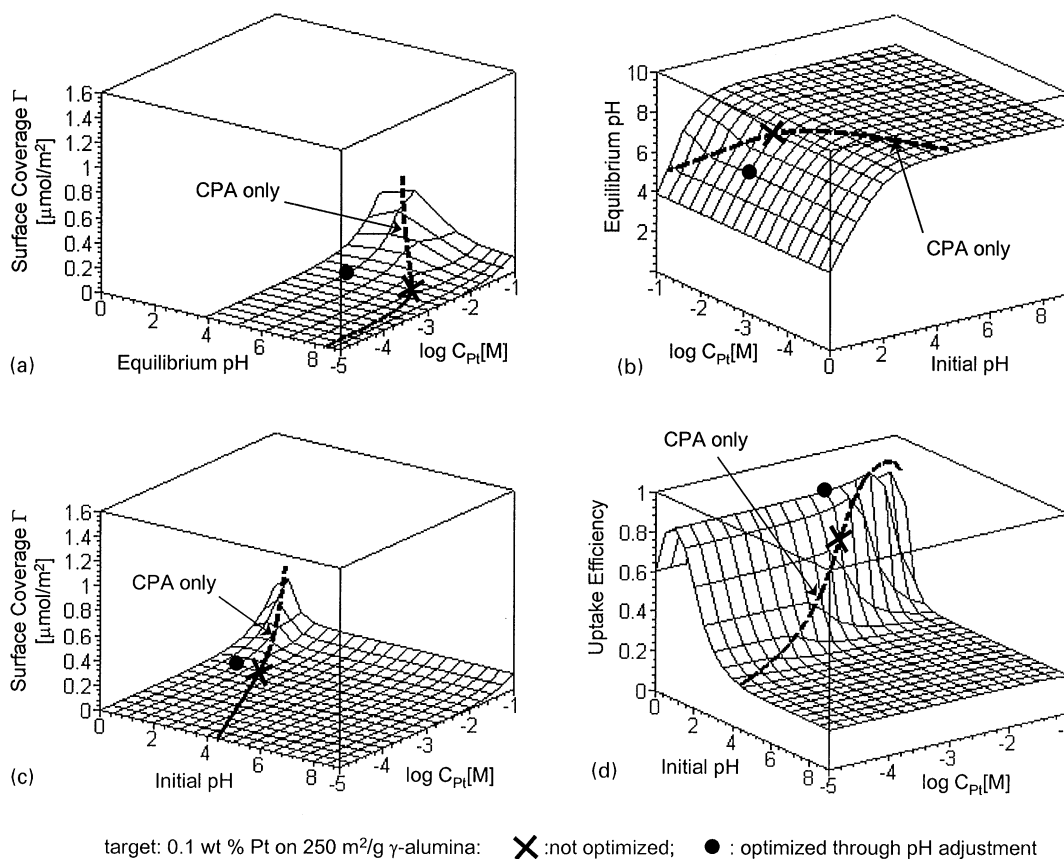


Fig. 12. Simulation of platinum adsorption and pH shift in a CPA/ $\gamma$ -alumina impregnation system at a surface loading of  $150\,000\text{ m}^2/\text{l}$ : (a) surface coverage vs. initial Pt concentration and equilibrium pH; (b) equilibrium pH vs. initial Pt concentration and initial pH; (c) surface coverage vs. initial Pt concentration and initial pH; (d) uptake efficiency vs. initial Pt concentration and initial pH.

Table 1  
Summary of the experimental impregnation parameters of the simulated data

Reference	Support	SA ( $\text{m}^2/\text{g}$ )	PZC	$N_s$ ( $1/\text{nm}^2$ )	$\Delta pK$	SL ( $\text{m}^2/\text{l}$ )	contact time (h)	$C_{\text{Pt,init}}$ ( $\text{mmol/l}$ )	Acid/Base
Mang et al.	$\gamma\text{-Al}_2\text{O}_3$ , crushed pellets	227	8.1	8	5	4540	1	5	HCl, NaOH
Papageorgiou et al.	$\gamma\text{-Al}_2\text{O}_3$ , powdered	78	8.5	8	5	11 760	1.5	0.37–7.9	—
Shyr and Ernst	$\gamma\text{-Al}_2\text{O}_3$ , pellets	150	8.5	8	5	33 000	2	6.9–57	—
Santacesaria et al.	$\gamma\text{-Al}_2\text{O}_3$ , powdered	177	8.5	8	5	2210	3–8	0.73–40	—
Jianguo et al.	$\eta\text{-Al}_2\text{O}_3$ , ground pellets	245	8.5	8	5	6125	6	4.3–29	—

offer an alternative interpretation of the role of excess HCl in the impregnation of pellets with homogeneous metal distribution at high surface loading (dry impregnation). While usually  $\text{Cl}^-$  is said to be necessary to “compete” with platinum for adsorption sites and thus drive it deeper into the pellet, our modeling results suggest that it is the additional protons that are required to sufficiently charge the large amounts of oxide surface and facilitate full platinum uptake.

The general formulation of the model makes it a promising tool for the optimization of catalyst impregnations for other, possibly less studied metal-support systems.

## Acknowledgements

The support of the UOP Research Center, Des Plaines, IL and the National Science Foundation (Grant #9908181) is gratefully acknowledged.

## Appendix

Input parameters for the RPA model are for all simulations in this study: radius of the unhydrated ion:  $2.95\text{ \AA}$  (CPA),  $2.41\text{ \AA}$  (TAPC); radius of a water molecule:  $1.35\text{ \AA}$ ; number of hydration sheaths: 1 (CPA), 2

Table 2  
Consideration of ionic strength in the simulations of the experimental data

References	Final pH	$C_{Pt,eq}$	Cl <sup>-</sup> ligand exchange	Cl <sup>-</sup> from acid	Na <sup>+</sup> from base	Dissolved Al <sub>3</sub> <sup>+</sup>
Mang et al.	Reported	Yes <sup>a</sup>	2Cl <sup>-</sup> /Pt	Yes <sup>b</sup>	Yes <sup>b</sup>	Yes <sup>c</sup>
Papageorgiou et al.	Simulated	Yes <sup>a</sup>	2Cl <sup>-</sup> /Pt	—	—	No <sup>d</sup>
Shyr and Ernst	Simulated	Yes <sup>a</sup>	2Cl <sup>-</sup> /Pt	—	—	No <sup>d</sup>
Santacessaria et al.	Simulated	Yes <sup>a</sup>	2Cl <sup>-</sup> /Pt	—	—	Yes <sup>c</sup>
Jianguo et al.	Simulated	Yes <sup>a</sup>	2Cl <sup>-</sup> /Pt	—	—	No <sup>d</sup>

<sup>a</sup>Platinum not adsorbed but left in solution is considered through recursive algorithm in the RPA model.

<sup>b</sup>Calculated from reported initial pH data.

<sup>c</sup>Data was reported, effect taken into account.

<sup>d</sup>Data was not reported, effect not taken into account.

(TAPC); temperature: 298.15 K; point of zero charge PZC: 8.5 (except Mang, see Table 1); surface ionization constants  $\Delta pK$ : 5; dielectric constant  $\epsilon$  for alumina: 14.2; hydroxyl site density  $N_s$ : 8 groups/nm<sup>2</sup>.

The following Tables 1 and 2 summarize all essential experimental parameters of the simulated studies and contributions to the ionic strength as they were taken into account in the RPA simulation:

## References

- Agashe, K., & Regalbuto, J. R. (1997). A revised physical theory for adsorption of metal complexes at oxide surfaces. *Journal of Colloidal and Interface Science*, 185, 174–189.
- Anderson, J. R. (1975). *Structure of Metallic Catalysts*. New York: Academic Press.
- Brunelle, J. P. (1978). Preparation of catalysts by adsorption of metal complexes on mineral oxides. *Pure and Applied Chemistry*, 50, 1211–1229.
- Chu, P., Peterson, E. E., & Radke, C. J. (1989). Modeling wet impregnation on  $\gamma$ -alumina. *Journal of Catalysis*, 117, 52–70.
- Contescu, C., & Vass, M. I. (1987). The effect of pH on the adsorption of palladium (II) complexes on alumina. *Applied Catalysis*, 33, 259–271.
- Cox, L. E., & Peters, D. E. (1970). Electronic and vibrational spectra for transdihydroxotetrachloroplatinate(IV). *Inorganic Chemistry*, 9, 1927–1930.
- D'Espinose de la Caillerie, J. -B., Kermarec, M., & Clause, O. (1995). Impregnation of  $\gamma$ -alumina with Ni(II) or Co(II) ions at neutral pH: Hydrotalcite-type coprecipitate formation and characterization. *Journal of American Chemical Society*, 117, 11471–11481.
- Davidson, C. M., & Jameson, R. F. (1965). Complexes formed between the platinum metals and halide ions. *Transactions of Faraday Society*, 61, 2462–2467.
- Davis, J. A., James, R. O., & Leckie, J. O. (1978). Surface ionization and complexation at the oxide/water interface. *Journal of Colloidal and Interface Science*, 63, 480–499.
- Gmelin, L., & Meyer, R. J. (1939). *Gmelins Handbuch der anorganischen Chemie*. Platin, Teil C Lieferung 1, 8. Auflage, Weinheim: Verlag Chemie.
- Hao, X., Spieker, W., & Regalbuto, J. R. (2001). A simplification of the revised physical adsorption model (in preparation).
- Healy, T. W., & White, L. R. (1978). Ionizable surface group models of aqueous interfaces. *Advances in Colloidal and Interface Science*, 9, 303–345.
- Healy, T. W., Yates, D. E., White, L. R., & Chan, D. (1977). Nernstian and non-Nernstian potential differences at aqueous interfaces. *Journal of Electroanalytical Chemistry*, 80, 57–66.
- Heise, F. J., & Schwarz, J. A. (1985). Preparation of metal distributions within catalyst support. I. Effect of pH on catalytic profiles. *Journal of Colloidal and Interface Science*, 107, 237–243.
- Heise, F. J., & Schwarz, J. A. (1986). Preparation of metal distributions within catalyst support. II. Effect of ionic strength on catalytic metal profiles. *Journal of Colloidal and Interface Science*, 113, 55–61.
- Heise, F. J., & Schwarz, J. A. (1987). In: A. Celmon, P. Grange, P. A. Jacobs, & G. Poncelet (Eds.), *Preparation of Catalysts IV* (pp. 1–13). Amsterdam: Elsevier.
- Heise, F. J., & Schwarz, J. A. (1988). Preparation of metal distributions within catalyst support. III. Single component modeling of pH, ionic strength and concentration effects. *Journal of Colloidal and Interface Science*, 123, 51–58.
- Heise, F. J., & Schwarz, J. A. (1990). Preparation of metal distributions within catalyst support. IV. Multicomponent effects. *Journal of Colloidal and Interface Science*, 135, 461–467.
- Huang, Y.-J. R., Barrett, B. T., & Schwarz, J. A. (1986). The effect of solution variables on metal weight loading during catalyst preparation. *Applied Catalysis*, 24, 241–248.
- James, R. O., & Healy, T. W. (1972a). Adsorption of hydrolysable metal ions at the oxide–water interface, I. Co (II) adsorption of SiO<sub>2</sub> and TiO<sub>2</sub> as model systems. *Journal of Colloidal and Interface Science*, 40, 42–52.
- James, R. O., & Healy, T. W. (1972b). Adsorption of hydrolysable metal ions at the oxide–water interface, II. Charge reversal of SiO<sub>2</sub> and TiO<sub>2</sub> colloids by adsorbed Co (II), La (III) and Th (IV) as model system. *Journal of Colloidal and Interface Science*, 40, 53–64.
- James, R. O., & Healy, T. W. (1972c). Adsorption of hydrolysable metal ions at the oxide–water interface, III. A thermodynamic model of adsorption. *Journal of Colloidal and Interface Science*, 40, 65–81.
- James, R. O., & Parks, G. A. (1982). Characterization of aqueous colloids by their electrical double-layer and intrinsic surface chemical properties. *Surface Colloidal Science*, 12, 119–216.
- Jianguo, W., Jiayu, Z., & Li, P. (1983). The role of competitive adsorbate in the impregnation of platinum in pelleted alumina support. In G. Poncelet, P. Grange, & P. A. Jacobs (Eds.), *Preparation of Catalysts III* (pp. 57–67). Amsterdam: Elsevier.
- Karakonstantis, L., Bourikas, K., & Lycourghiotis, A. (1996). Tungsten-oxo-species deposited on alumina. 1. Investigation of the nature of the tungstates deposited on the interface of the gamma-alumina/electrolyte solutions at various pH's. *Journal of Catalysis*, 162, 295–305.

- Lee, S.-Y., & Aris, R. (1985). The distribution of active ingredients in supported catalysts prepared by impregnation. *Catalytic Review of Science and Engineering*, 27, 207–340.
- Luengo, M. A., Sermon, P. A., & Sing, K. S. W. (1987). In B. Delmon, P. Grange, P. A. Jacobs, & G. Poncelet (Eds.), *Preparation of Catalysts IV* (pp. 29–43). Amsterdam: Elsevier.
- Maatman, R. W. (1959). How to make a more effective catalyst. *Industrial Engineering Chemistry*, 51, 913–914.
- Mang, T., Breitscheidel, B., Polanek, P., & Knözinger, H. (1993). Adsorption of platinum complexes on silica and alumina: preparation of non-uniform metal distributions within support pellets. *Applied Catalysis A: General*, 106, 239–258.
- Noh, J. S., & Schwarz, J. A. (1990). Estimation of surface ionization constants for amphoteric solids. *Journal of Colloidal and Interface Science*, 139, 139–148.
- Papageorgiou, P., Price, D. M., Gavriilidis, A., & Varma, A. (1996). Preparation of Pt/ $\gamma$ -Al<sub>2</sub>O<sub>3</sub> pellets with internal step distribution of catalyst: Experiments and theory. *Journal of Catalysis*, 158, 439–451.
- Park, J., & Regalbuto, J. R. (1995). A simple, accurate determination of oxide PZC and the strong buffering effect of oxide surfaces at incipient wetness. *Journal of Colloidal and Interface Science*, 175, 239–252.
- Regalbuto, J. R., Agashe, K., Navada, A., Bricker, M. L., & Chen, Q. (1998). A scientific description of Pt adsorption onto alumina. *Studies in Surface Science and Catalysis*, 118, 147–156.
- Regalbuto, J. R., Navada, A., Shadid, S., Bricker, M. L., & Chen, Q. (1999). An experimental verification of the physical nature of Pt adsorption onto alumina. *Journal of Catalysis*, 184, 335–348.
- Ruckenstein, E., & Karpe, P. (1989). Control of metal distribution in supported catalysts by pH, ionic strength and coimpregnation. *Langmuir*, 5, 1393–1407.
- Santacessaria, E., Carra, S., & Adami, I. (1977). Adsorption of Hexachloroplatinic acid on  $\gamma$ -alumina. *Industrial Engineering Chemistry and Production Research Development*, 16, 41–47.
- Santhanam, N., Conforti, T. A., Spieker, W. A., & Regalbuto, J. R. (1994). Nature of metal catalyst precursors adsorbed onto oxide supports. *Catalysis Today*, 21, 141–156.
- Shah, A., & Regalbuto, J. R. (1994). Retardation of Pt adsorption over oxide supports at pH extremes: oxide dissolution or high ionic strength. *Langmuir*, 10, 500–504.
- Shyr, Y., & Ernst, W. (1980). Preparation of nonuniformly active catalysts. *Journal of Catalysis*, 63, 425–432.
- Sillen, L. G., & Martell, A. E. (1971). *The Stability Constants of Metal Ion Complexes*. Special Publication No. 25 (Suppl. No. 1), Burlington House, London: The Chemical Society.
- Smirnova, I. E., Belyi, A. S., Smolikov, M. D., & Dublyakin, V. K. (1990). Distribution of the active component over pores of different size in the structure of oxide supports. IV. The effect of impregnation conditions on the platinum distribution in the porous structure of alumina. *Kinetic Catalyses*, 31, 602–606.
- Spieker, W. A., Regalbuto, J. R., Kropf, J., & Miller, J. T. (in preparation).
- Summers, J. C., & Ausen, S. A. (1978). Catalyst impregnation: reaction of noble metal complexes with alumina. *Journal of Catalysis*, 52, 445–452.
- Szeica, O. A., Castro, A. A., Dario, R. A., & Parera, J. M. (1986). Modeling of the impregnation step to prepare supported Pt/Al<sub>2</sub>O<sub>3</sub> catalysts. *Industrial Engineering Chemistry Fundamentals*, 25, 84–88.
- Vincent, R. C., & Merrill, R. P. (1974). Concentration profiles in impregnation of porous catalysts. *Journal of Catalysis*, 35, 206–217.
- Wiese, G. R., James, R. O., & Healy, T. W. (1971). Discreteness of charge and solvation effects in cation adsorption at oxide/water interfaces. *Chem. Society of London, Faraday Discussion*, 50, 302–311.
- Xidong, W., Yongnian, Y., & Jiayu, Z. (1988). Influence of soluble aluminum on the state and surface properties of platinum in a series of reduced platinum/alumina catalysts. *Applied Catalysis*, 40, 291–313.
- Yates, D. E., Levine, S., & Healy, T. W. (1974). Site-binding model of the electric double layer at the oxide/water interface. *Journal of Chemical Society and Faraday Transactions*, 70, 1807–1818.